

Robust Auxiliary-Noise-Power Scheduling in Active Noise Control Systems With Online Secondary Path Modeling

Shakeel Ahmed, *Student Member, IEEE*, Muhammad Tahir Akhtar, *Senior Member, IEEE*, and Xi Zhang, *Senior Member, IEEE*

Abstract—This paper deals with the auxiliary noise-based methods for active noise control (ANC) systems with online secondary path modeling (SPM). The proposed method comprises two adaptive filters: the modified Filtered-X normalized least-mean-square algorithm-based ANC filter, and the normalized least-mean-square algorithm-based SPM filter excited by auxiliary noise. The auxiliary noise injected for online SPM, degrades the noise-reduction performance of the ANC system. A two-stage gain scheduling strategy is proposed to vary power of the auxiliary noise. In the first stage the gain is varied on the basis of power of the error signal of SPM filter, and in the second stage the gain is varied on the basis of the correlation estimate of the two adjacent samples of the error signal of SPM filter. The main idea is to inject large-power auxiliary noise at the start up or when a change in the acoustic paths is detected, and to reduce the power as the system converges. The proposed method achieves a fast convergence of the SPM filter and gives a robust performance in the presence of strong perturbation in acoustic paths. Furthermore, the proposed method improves the noise-reduction performance at steady-state even in the presence of an uncorrelated disturbance at the error microphone. Moreover, the improved performance is achieved at a lower computational cost as compared with a recent method proposed in [A. Carini, and S. Malatini, “Optimal variable step-size NLMS algorithms with auxiliary noise power scheduling for feedforward active noise control,” *IEEE Trans. Audio, Speech Lang. Process.*, vol. 16, no. 8, pp. 1383–1395, Nov. 2008]. Extensive simulations are carried out to verify the effectiveness of the proposed method.

Index Terms—Active noise control (ANC), auxiliary-noise-power scheduling, online secondary path modeling.

I. INTRODUCTION

ACTIVE noise control (ANC) systems are employed for attenuating the low frequency acoustic noise by generating an anti-noise with the help of a controlled secondary source (loudspeaker) [1], [2]. In ANC systems, the most widely used adaptive algorithm is Filtered-X-LMS (FXLMS) algorithm [3], due to its robustness. The implementation of FXLMS algorithm requires the secondary path model $\hat{s}(n)$ (see Fig. 1). The effect

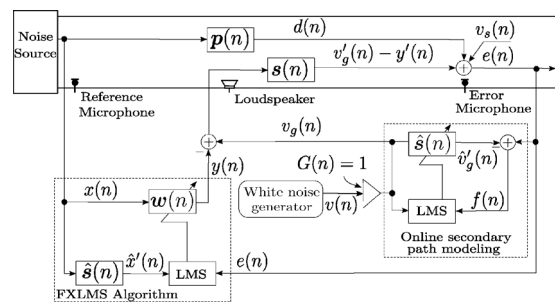


Fig. 1. Block diagram of Eriksson's method for ANC systems with online secondary path modeling.

of estimation error in model of secondary path on the performance of FXLMS algorithm is studied in [3]–[7]. This model can be obtained offline, however, online modeling is needed to cope with the time-varying nature of acoustic paths. The basic method for ANC systems with online secondary path modeling (SPM) is proposed by Eriksson *et al.*. The block diagram of Eriksson's method [8] is shown in Fig. 1, where $x(n)$ is the input reference signal picked by the reference microphone, $e(n)$ is the residual error signal measured by the error microphone, $p(n)$ denotes the impulse response vector for the primary path from the reference microphone to the error microphone, $w(n)$ represents the impulse response vector of ANC filter, $s(n)$ is the impulse response vector for the secondary path from output of $w(n)$ to the error microphone, $\hat{s}(n)$ is the impulse response vector of SPM filter, and $y(n) = w(n) * x(n)$ is the output of $w(n)$, where $*$ represents the convolution operation. In order to account for 180° phase shift, the sign of $y(n)$ is changed before it is applied to the input of $s(n)$.

Assuming $v_s(n) = 0$, the residual error signal at the error microphone, $e(n)$, is given as

$$e(n) = (d(n) - y'(n)) + v_g'(n), \quad (1)$$

where $d(n) = p(n) * x(n)$ is the output of $p(n)$, $y'(n) = s(n) * y(n)$, and $v_g'(n) = s(n) * v_g(n)$ are outputs of $s(n)$ corresponding to input $y(n)$ and $v_g(n)$, respectively, $v_g(n) = G(n)v(n)$ where $G(n)$ is the time-varying gain to control power of $v_g(n)$ and $v(n)$ is auxiliary white gaussian noise (WGN) signal which is uncorrelated with $x(n)$. In Eriksson's method $G(n) = 1$, and block for $G(n)$ is included in Fig. 1 for consistency with other block diagrams in the paper. The error signal of $\hat{s}(n)$, $f(n)$, is computed as

$$f(n) = e(n) - \hat{v}_g'(n) = (d(n) - y'(n)) + (v_g'(n) - \hat{v}_g'(n)), \quad (2)$$

where $\hat{v}_g'(n) = \hat{s}(n) * v_g(n)$ is output of $\hat{s}(n)$.

A fixed power auxiliary noise (note $G(n) = 1$ in Eriksson's method) degrades the noise-reduction performance of ANC

Manuscript received April 23, 2012; revised August 15, 2012; accepted November 18, 2012. Date of publication December 20, 2012; date of current version January 18, 2013. This work was supported by MEXT research scholarship, government of Japan. The associate editor coordinating the review of this manuscript and approving it for publication was Prof. Boaz Rafaely.

S. Ahmed and X. Zhang are with the Department of Communication Engineering and Informatics, The University of Electro-Communications, Chofu, Tokyo 182-8585, Japan (e-mail: shakeel@uec.ac.jp; zhangxi@uec.ac.jp).

M. T. Akhtar is with The Center for Frontier Science and Engineering (CFSE), The University of Electro-Communications, Chofu, Tokyo 182-8585, Japan (e-mail: akhtar@uec.ac.jp).

Color versions of one or more of the figures in this paper are available online at <http://ieeexplore.ieee.org>.

Digital Object Identifier 10.1109/TASL.2012.2234112

system at steady-state. The improvements in Eriksson's method can be found in [9]–[20]. As in Eriksson's method, the methods proposed in [9]–[12] use auxiliary noise with fixed variance in all operating conditions. In order to achieve the conflicting requirements of fast convergence of $\hat{s}(n)$ and reduced residual error power in steady-state, a strategy for auxiliary-noise-power (ANP) scheduling is proposed in [13] for frequency domain ANC systems. In [14], ANP is varied on the basis of convergence status of the ANC system and the power of input reference signal. In [15], Akhtar *et al.* extended their previous work [12] and incorporated a strategy for ANP scheduling to improve the noise-reduction performance. Recently, Carini *et al.*, proposed a self-tuning strategy for ANP scheduling [16], and employed this strategy along with the optimal normalized step-size parameters for the adaptive filters $w(n)$ and $\hat{s}(n)$ [17]. The analysis of online SPM with ANP scaled by one-sample-delayed residual error signal is given in [18]. A novel On/Off switching strategy for auxiliary noise is proposed in [19] where injection of the auxiliary noise is suspended after convergence of $\hat{s}(n)$, and is resumed when perturbation in acoustic paths is detected. In [20], two methods are proposed for ANP variation. The first method improves the On/Off switching strategy of [19] by reducing the number of empirically selected threshold parameters, and gives a clear criterion for suspending/resuming the injection of auxiliary noise. The second method in [20] can effectively track the variations in acoustic paths, however, the gain is upper bounded by the input reference signal power, and ANC system may become unstable for strong perturbations in the acoustic paths. In this paper we propose a new gain scheduling strategy to vary ANP, which

- 1) improves the convergence speed of the $\hat{s}(n)$,
- 2) improves the noise-reduction performance of ANC system in steady-state,
- 3) improves the performance of ANC system in the presence of uncorrelated WGN at error sensor,
- 4) makes the ANC system more robust, so that it should remain stable even for very strong perturbations in acoustic paths, and
- 5) reduces the computational cost of the algorithm compared to Carini's method.

The rest of the paper is organized as follows. Section II gives a brief overview of Carini's method, and Section III contains the description of the proposed method and computational complexity analysis. Section IV explains the simulation results followed by the concluding remarks given in Section V.

II. EXISTING METHOD

A. Carini's Method

The block diagram of Carini's method is shown in Fig. 2, where: 1) a self-tuning ANP scheduling strategy is proposed, 2) optimal normalized step-size parameters are employed for adaptation of $w(n)$ and $\hat{s}(n)$, and to estimate optimal value of step-size $\mu_s(n)$ for $\hat{s}_A(n)$, a delay-coefficient technique [21] based on delay D is employed. In Fig. 2, $\hat{s}_A(n) = [\hat{s}_0(n) \ \hat{s}(n)]^T$ is a vector of length $D + L_s$, where D and L_s are the lengths of $\hat{s}_0(n)$, and $\hat{s}(n)$, respectively.

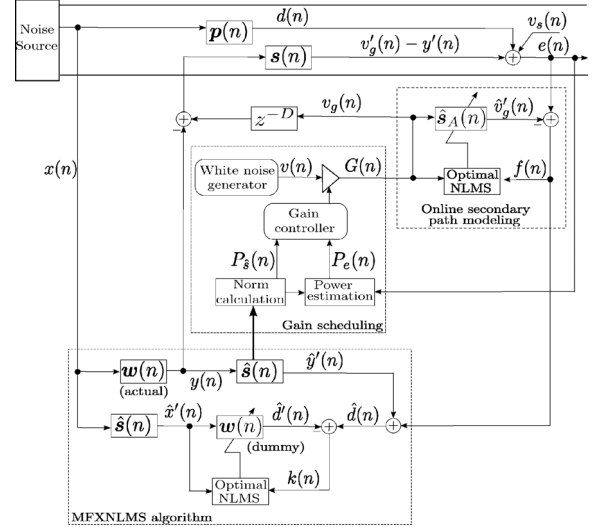


Fig. 2. Block diagram of Carini's method for ANC systems with online secondary path modeling.

The self-tuning ANP scheduling strategy is such that the ratio $R(n)$ given by

$$R(n) = \frac{E[(d(n) - y'(n))^2]}{E[(v'_g(n))^2]} = \text{constant} \quad \forall n, \quad (3)$$

is kept constant in every operating conditions, where $E[\cdot]$ is the expectation operator. The gain, $G(n)$, is computed as

$$G(n) = \sqrt{\frac{P_e(n)}{(R+1)P_s(n)}}, \quad (4)$$

where powers $P_e(n)$ and $P_s(n)$ are estimated using low pass estimator, respectively, as

$$P_e(n) = \lambda P_e(n-1) + (1-\lambda)e^2(n), \quad (5)$$

$$P_s(n) = \lambda P_s(n-1) + (1-\lambda)\hat{s}^T(n)\hat{s}(n), \quad (6)$$

where $0.9 < \lambda < 1$ is a forgetting factor.

A heuristic approach is used to estimate the optimal step-size parameter, $\mu_w(n)$, as

$$\mu_w(n) = \frac{\hat{N}_w(n)}{P_k(n)(\hat{\mathbf{x}}'^T(n)\hat{\mathbf{x}}'(n))}, \quad (7)$$

where $\hat{\mathbf{x}}'(n) = [\hat{x}'(n), \hat{x}'(n-1), \dots, \hat{x}'(n-L_w+1)]^T$ is the input filtered-reference signal vector, L_w is the filter tap-weight length, $\hat{x}'(n) = \hat{s}(n) * x(n)$ is the filtered-reference signal, $P_k(n)$ is the power of the error signal $k(n)$ that can be obtained by using estimator of type (5), and $\hat{N}_w(n)$ is computed as

$$\hat{N}_w(n) = \lambda \hat{N}_w(n-1) + (1-\lambda)k(n)\hat{\mathbf{m}}^T(n)\hat{\mathbf{x}}'(n), \quad (8)$$

where $\hat{\mathbf{m}}(n)$ is computed as

$$\hat{\mathbf{m}}(n) = \hat{\lambda}\hat{\mathbf{m}}(n-1) + \frac{(1-\hat{\lambda})k(n)\hat{\mathbf{x}}'(n)}{\hat{\mathbf{x}}'^T(n)\hat{\mathbf{x}}'(n)}, \quad (9)$$

and $\hat{\lambda}$ is selected in the range [0.6, 0.9].

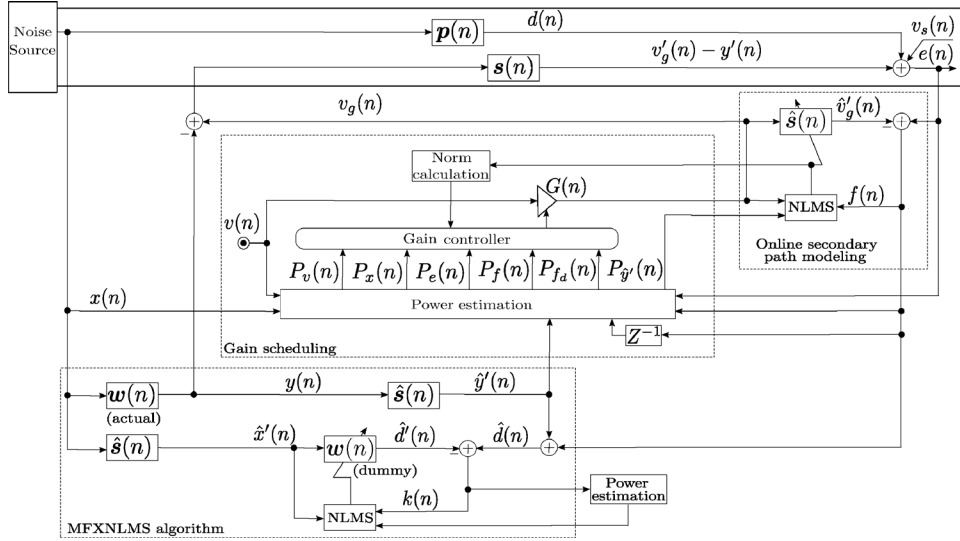


Fig. 3. Block diagram of the proposed method with novel strategy for auxiliary noise power scheduling in ANC systems with online secondary path modeling.

Finally, the step-size parameter $\mu_s(n)$ for extended length modeling filter $\hat{\mathbf{s}}_A(n)$ is computed as

$$\mu_s(n) = \begin{cases} \frac{\hat{N}_s(n)}{P_f(n)(\mathbf{v}_{g(L_s+D)}^T(n)\mathbf{v}_{g(L_s+D)}(n))}; & \frac{\hat{N}_s(n)}{P_f(n)} > \mu_{s_{\min}} \\ \frac{\mu_{s_{\min}}}{\mathbf{v}_{g(L_s+D)}^T(n)\mathbf{v}_{g(L_s+D)}(n)}; & \text{otherwise} \end{cases} \quad (10)$$

where

$$\hat{N}_s(n) = \lambda \hat{N}_s(n-1) + \frac{1-\lambda}{D} \left(\hat{\mathbf{s}}_0^T(n) \hat{\mathbf{s}}_0(n) \mathbf{v}_{g(L_s+D)}^T(n) \mathbf{v}_{g(L_s+D)}(n) \right), \quad (11)$$

and $\mathbf{v}_{g(L_s+D)}(n) = [v_g(n), v_g(n-1), \dots, v_g(n-L_s-D+1)]^T$ is the input signal vector of $\hat{\mathbf{s}}_A(n)$.

A few remarks regarding Carini's method are given below:

- The first part of $\hat{\mathbf{s}}_A(n)$, i.e., $\hat{\mathbf{s}}_0(n)$, is to model the artificially introduced delay z^{-D} , so after the convergence of ANC system, the term $\hat{\mathbf{s}}_0^T(n)\hat{\mathbf{s}}_0(n)$ in (11) is very small (ideally zero). The perturbation in acoustic paths would cause an increase in the power of $f(n)$, so the term $P_f(n)$ in the denominator of (10) will drive the condition $\hat{N}_s(n)/P_f(n) > \mu_{s_{\min}}$ to be false, and hence the step-size for $\hat{\mathbf{s}}_A(n)$ will be determined by $\mu_{s_{\min}}/(\mathbf{v}_{g(L_s+D)}^T(n)\mathbf{v}_{g(L_s+D)}(n))$. The step-size for SPM filter stays at small value even if there is a perturbation in the acoustic paths, thus resulting in a poor tracking performance. Here $\mu_{s_{\min}}$ is used to avoid freezing completely the adaptation in these conditions.
- The ratio $R(n)$ in (3) is constant in all operating conditions (The value of the constant is selected as 1 for Carini's method). This means, that $E[(v'_g(n))^2] = E[(d(n) - y'(n))^2]$ is always satisfied. From Fig. 2, $E[(v'_g(n))^2] = G^2(n)\|\mathbf{s}(n)\|^2 E[v^2(n)]$, therefore the gain $G(n)$ at steady-state is proportional to $\sqrt{E[(d(n) - y'(n))^2]}$. After the convergence of ANC system: 1) the step-size for $\hat{\mathbf{s}}_A(n)$ is determined by $\mu_{s_{\min}}/(\mathbf{v}_{g(L_s+D)}^T(n)\mathbf{v}_{g(L_s+D)}(n))$, and 2) the input signal

power for $\hat{\mathbf{s}}_A(n)$ is determined by the $E[(d(n) - y'(n))^2]$. These two conditions results in slow convergence of SPM filter, when there is a perturbation in the acoustic paths.

- The presence of uncorrelated disturbance, $v_s(n)$, at the error microphone contributes to the power of residual error signal, $P_e(n)$. The signal $v_s(n)$ with large variance results in large value of the gain $G(n)$ (see (4)), thus degrades the noise-reduction performance.
- The overall computational complexity of Carini's method is very high. The high computational cost is mainly due to the online estimation of optimal normalized step-size parameters for ANC filter and SPM filter.

III. PROPOSED METHOD

The block diagram of the proposed method is shown in Fig. 3, where a delay z^{-1} , power estimation, norm calculation, and gain controller blocks are used to realize the proposed ANP scheduling strategy. From (1), $E[e^2(n)]$ can be written as follows

$$E[e^2(n)] = E[(d(n) - y'(n))^2] + E[(v'_g(n))^2], \quad (12)$$

where

$$E[(v'_g(n))^2] = G^2(n)\|\mathbf{s}(n)\|^2 E[v^2(n)] = G^2(n)\|\mathbf{s}(n)\|^2, \quad (13)$$

where $E[v^2(n)] = 1$, (note that $v(n)$ is a zero-mean unit variance WGN). It is evident from (12) and (13) that the time-varying gain $G(n)$ can be employed to control the contribution of $E[(v'_g(n))^2]$ to $E[e^2(n)]$. In the proposed approach the gain $G(n)$ is computed such that the ratio $R(n)$ (defined in (3)) is time-varying. As long as $\hat{\mathbf{s}}(n)$ is away from $\mathbf{s}(n)$, the ratio $R(n)$ is lower than 0 dB guaranteeing fast convergence of SPM filter. The fast convergence of SPM filter is desirable, because accurate model of $\mathbf{s}(n)$ is needed for modified Filtered-X normalized least-mean-square (MFXNLMS) algorithm-based adaptation of ANC filter. After convergence of the SPM filter, $R(n)$ becomes greater than 0 dB ensuring that

$E[(v'_g(n))^2] < E[(d(n) - y'(n))^2]$, which in turn improves the noise-reduction performance.

A. Gain Scheduling Strategy of the Proposed Method

We propose a two-stage strategy to compute the time-varying gain, $G(n)$.

Stage 1: When the ANC system is far from steady-state i.e., when $P_f(n) > P_x(n)$. This situation can occur

- at the start-up of ANC system, and
- when there is a strong perturbation in the acoustic paths.

Stage 2: When the ANC system is close to steady-state i.e., when $P_f(n) \leq P_x(n)$.

The subsequent subsections will explain each of these stages one by one.

Stage 1: $P_f(n) > P_x(n)$, when the ANC system is far from steady-state.

The error signal, $f(n)$ (see (2)), of $\hat{\mathbf{s}}(n)$ has two parts: first part $d(n) - y'(n)$ carries information about the convergence of the ANC filter $\mathbf{w}(n)$, and acts as an interference to the adaptation of the SPM filter. The second part $v'_g(n) - \hat{v}'_g(n)$ plays exactly reverse role, i.e., carries information about the convergence of $\hat{\mathbf{s}}(n)$ and acts as an interference for $\mathbf{w}(n)$. The power of the error signal of $\hat{\mathbf{s}}(n)$, $f(n)$, can be written as:

$$P_f(n) = P_{d-y'}(n) + P_{v'_g-\hat{v}'_g}(n), \quad (14)$$

where $P_{d-y'}(n)$ denotes the estimate of the power of interference term $d(n) - y'(n)$ in the error signal of $\hat{\mathbf{s}}(n)$, and $P_{v'_g-\hat{v}'_g}(n)$ denotes the estimate of the power of the desired term $v'_g(n) - \hat{v}'_g(n)$ in the error signal of $\hat{\mathbf{s}}(n)$. At this stage, the interference term $d(n) - y'(n)$ for $\hat{\mathbf{s}}(n)$ is strong, therefore the gain $G(n)$ is varied in accordance with 1) the convergence status of $\mathbf{w}(n)$ (power of interference term $P_{d-y'}(n)$), 2) the convergence status of $\hat{\mathbf{s}}(n)$, and is computed by making the power $P_{v'_g-\hat{v}'_g}(n)$ to be equal to the power $P_f(n-1)$. In the case of ANC systems, the signal $v'_g(n)$ is not accessible, therefore the following condition

$$P_{\hat{v}'_g}(n) = P_f(n-1), \quad (15)$$

is forced, where $P_f(n-1)$ is estimated online using estimator of type (5), and $P_{\hat{v}'_g}(n)$ can be expressed as

$$P_{\hat{v}'_g}(n) \approx G^2(n) \|\hat{\mathbf{s}}(n)\|^2 E[v^2(n)] = G^2(n) \|\hat{\mathbf{s}}(n)\|^2. \quad (16)$$

Equating the right hand sides of (15) and (16), and solving for $G(n)$, we get

$$G(n) = \sqrt{\frac{P_f(n-1)}{\|\hat{\mathbf{s}}(n)\|^2}} = \sqrt{\frac{P_{d-y'}(n-1) + P_{v'_g-\hat{v}'_g}(n-1)}{\|\hat{\mathbf{s}}(n)\|^2}}. \quad (17)$$

As long as $\hat{\mathbf{s}}(n)$ is away from $\mathbf{s}(n)$, the gain $G(n)$ will keep on increasing due to the presence of the term $P_{v'_g-\hat{v}'_g}(n-1)$ in $P_f(n-1)$. This will ensure fast convergence of $\hat{\mathbf{s}}(n)$ and result in the ratio $R(n) < 0$ dB. When $\hat{\mathbf{s}}(n) \rightarrow \mathbf{s}(n)$, $\hat{v}'_g(n) \rightarrow v'_g(n)$, and $f(n) \rightarrow (d(n) - y'(n))$, the positive feedback scenario for the gain $G(n)$ will automatically breakup and the ratio $R(n) \rightarrow 0$ dB.

Stage 2: $P_f(n) \leq P_x(n)$, when the ANC system is close to steady-state.

If only (17) is used for computing gain, $G(n)$, then the maximum performance we can achieve in steady-state can result in $R(n) = 0$ dB. However, to have improved noise-reduction performance in steady-state, it is desirable to have $R(n) > 0$ dB. When the condition $P_f(n) \leq P_x(n)$ is satisfied, the ANC system is close to steady-state, and in this case the gain $G(n)$ is computed as

$$G(n) = \begin{cases} \sqrt{\frac{P_x(n)}{P_v}}; & \beta(n) > \frac{P_x(n)}{P_v} \\ \beta(n); & \text{otherwise,} \end{cases} \quad (18)$$

where P_v denotes the power of $v(n)$, which is a positive constant set to one, and the time-varying parameter $\beta(n)$ is computed as

$$\beta(n) = \alpha\beta(n-1) + \gamma(n) \left(\frac{P_{f_d}(n)}{P_v} \right)^2, \quad (19)$$

where $0 < \alpha < 1$ and $\gamma(n) > 0$ are controlling parameters, and $P_{f_d}(n)$ is the estimate of $E[f(n)f(n-1)]$ (autocorrelation between $f(n)$ and $f(n-1)$) being computed as

$$\begin{aligned} E[f(n)f(n-1)] \\ \approx P_{f_d}(n) = \lambda P_{f_d}(n-1) + (1-\lambda)f(n)f(n-1). \end{aligned} \quad (20)$$

When switching occurs from first stage of gain scheduling to second stage, the condition $\beta(n) > (P_x(n)/P_v)$ may be true. In such a situation if we make $G(n) = \beta(n)$ then a large value of $\beta(n)$ will result in large value of $G(n)$, thus resulting in a large value of the interference term $(v'_g(n) - \hat{v}'_g(n))$ in the error signal of $\mathbf{w}(n)$. This may result in the divergence of $\mathbf{w}(n)$ and hence the whole ANC system. In order to avoid such a situation the value of the $G(n)$ is upper bounded by the input reference signal power, $P_x(n)$, until the condition $\beta(n) > (P_x(n)/P_v)$ is false; otherwise the gain will follow the variation of $\beta(n)$.

In the presence of an uncorrelated disturbance $v_s(n)$ at the error microphone $E[f(n)f(n-1)]$ can be expressed as

$$\begin{aligned} E[f(n)f(n-1)] \\ = E[(d(n) - y'(n))(d(n-1) - y'(n-1))] \\ + E[(v'_g(n) - \hat{v}'_g(n))(v'_g(n-1) - \hat{v}'_g(n-1))] \\ + E[v_s(n)v_s(n-1)]. \end{aligned} \quad (21)$$

where $E[v_s(n)v_s(n-1)] = 0$ as $v_s(n)$ is assumed as zero mean WGN. Thus the correlation $E[f(n)f(n-1)]$, and hence $P_{f_d}(n)$ is independent of the uncorrelated disturbance signal $v_s(n)$. In (21) a delay of at least L_s samples is needed for correlation term corresponding to $v(n)$ to vanish [10]. It is worth mentioning that, in the presence of an uncorrelated disturbance $v_s(n)$, the gain $G(n)$ computed using instantaneous energy of the signal $f(n)$ has large steady-state value [22]. Therefore employing $P_{f_d}(n)$ in computing $\beta(n)$ and hence gain $G(n)$ results in small steady-state gain even in the presence of $v_s(n)$ at the error microphone.

For a typical simulation the effect of $\gamma(n)$ on the modeling error $\Delta S(n)$ (as defined later in (30)) and ANP $E[(v'_g(n))^2]$

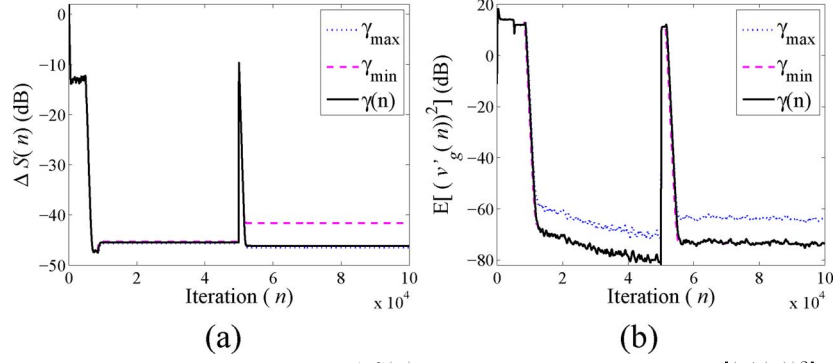


Fig. 4. Effect of different values of γ on (a) Relative modeling error, $\Delta S(n)$ (dB) (b) Auxiliary-noise-power, $E[(v'_g(n))^2]$ (dB): $\gamma_{\max} = 0.9$, $\gamma_{\min} = 0.3$, $\gamma(n)$ as defined in (22). (At $n = 5 \times 10^4$, there is a perturbation in acoustic paths).

is studied in Fig. 4. If there is a perturbation in the acoustic paths, large value of $\gamma(n)$ is desirable to have good modeling accuracy. However a large value of $\gamma(n)$ at steady-state would result in a large value for $E[(v'_g(n))^2]$, and thus degrades the noise-reduction performance (see (12)). On the other hand, a small value of $\gamma(n)$ reduces the contribution of $E[(v'_g(n))^2]$, but the performance is not good in terms of $\Delta S(n)$. In order to meet the conflicting requirements of a small steady-state value for $E[(v'_g(n))^2]$, and a good modeling accuracy, the value of $\gamma(n)$ in (19) is made adaptive and is computed as

$$\gamma(n) = \rho(n)\gamma_{\min} + (1 - \rho(n))\gamma_{\max}, \quad (22)$$

where $\rho(n) = P_f(n)/P_e(n)$ and is varying between 0 and 1 (the variation of $\rho(n)$ is explained later). In steady-state, $\rho(n) \rightarrow 1 \Rightarrow \gamma(n) \rightarrow \gamma_{\min}$, resulting in lower steady-state value of $E[(v'_g(n))^2]$, and hence improving the noise-reduction performance. Any perturbation in the acoustic paths would cause $\rho(n) \rightarrow 0$, and hence $\gamma(n) \rightarrow \gamma_{\max}$.

B. Variation of $\rho(n)$ in the Proposed Method

For all methods discussed in this paper, a two phase of operation is considered. In the first phase, $\mathbf{w}(n)$ is in a sleep state and only $\hat{\mathbf{s}}(n)$ is active. In the second phase, both $\mathbf{w}(n)$ and $\hat{\mathbf{s}}(n)$ are in operation.

- First phase (only SPM filter is active)

In the first phase, the output $y(n) = 0$, (as $\mathbf{w}(n)$ is in sleep state), therefore, $\rho(n)$ can be expressed as

$$\rho(n) = \frac{P_f(n)}{P_e(n)} = \frac{E[(d(n))^2] + E[(v'_g(n) - \hat{v}'_g(n))^2]}{E[(d(n))^2] + E[(v'_g(n))^2]}. \quad (23)$$

At the start-up of ANC system, $\rho(0) = P_f(0)/P_e(0) = 1$, and as the SPM filter converges $\hat{\mathbf{s}}(n) \rightarrow \mathbf{s}(n) \Rightarrow \hat{v}'_g(n) \rightarrow v'_g(n)$, and hence value of $\rho(n)$ decreases. The value of $\rho(n)$ at the end of first phase depends upon the duration of the initial phase, and the primary residual noise power, $E[(d(n))^2]$.

- Second phase (both $\hat{\mathbf{s}}(n)$ and $\mathbf{w}(n)$ are active).

In this phase both adaptive filters $\hat{\mathbf{s}}(n)$ and $\mathbf{w}(n)$ are in operation, and hence $\rho(n)$ can be expressed as

$$\rho(n) = \frac{P_f(n)}{P_e(n)} = \frac{E[(d(n) - y'(n))^2] + E[(v'_g(n) - \hat{v}'_g(n))^2]}{E[(d(n) - y'(n))^2] + E[(v'_g(n))^2]}. \quad (24)$$

where $E[(v'_g(n) - \hat{v}'_g(n))^2] < E[(v'_g(n))^2]$, and $E[(d(n) - y'(n))^2]$ decreases as $\mathbf{w}(n)$ converges. As stated earlier, the

gain $G(n)$ will keep on increasing as long as $\hat{\mathbf{s}}(n)$ is far from $\mathbf{s}(n)$. This situation can occur at the start-up of ANC system or when there is a perturbation in the acoustic paths. The positive feedback action for the gain $G(n)$ results in $E[(v'_g(n))^2] > E[(d(n) - y'(n))^2]$ ($R(n) < 0$ dB). This will result in a fast convergence of the SPM filter, and $\rho(n)$ decreases towards zero (see (24)). A kind of positive feedback scenario for the gain $G(n)$ will break up automatically when $\hat{\mathbf{s}}(n) \approx \mathbf{s}(n)$, because now the term $v'_g(n)$ will be cancelled out by $\hat{v}'_g(n)$. After the convergence of $\hat{\mathbf{s}}(n)$, the gain $G(n)$ reduces to a much lower value resulting in $E[(v'_g(n))^2] \ll E[(d(n) - y'(n))^2]$, and $E[(v'_g(n) - \hat{v}'_g(n))^2] \ll E[(d(n) - y'(n))^2]$, so $P_f(n) \rightarrow P_e(n)$, and hence, $\rho(n)$ in steady-state is given as

$$\lim_{n \rightarrow \infty} \rho(n) = \frac{P_f(n)}{P_e(n)} \approx \frac{E[(d(n) - y'(n))^2]}{E[(d(n) - y'(n))^2]} \approx 1. \quad (25)$$

C. Step-Size Variation

In contrast to Carini's method, in the proposed method normalized step-sizes (instead of optimal normalized step-sizes) are employed for $\mathbf{w}(n)$ and $\hat{\mathbf{s}}(n)$. This reduces the computations required to estimate the optimal step-size parameters. The weight update equation for $\mathbf{w}(n)$ is given by

$$\mathbf{w}(n+1) = \mathbf{w}(n) + \mu_w(n)k(n)\hat{\mathbf{x}}'(n), \quad (26)$$

where $\hat{\mathbf{x}}'(n) = [\hat{x}'(n), \hat{x}'(n-1), \dots, \hat{x}'(n-L_w+1)]^T$ is the input filtered-reference signal vector, $\hat{x}'(n) = \hat{\mathbf{s}}(n) * x(n)$ is the output of $\hat{\mathbf{s}}(n)$ for input $x(n)$, $k(n)$ is the error signal, and $\mu_w(n)$ is the normalized step-size parameter being computed as

$$\mu_w(n) = \frac{\mu_1}{\hat{\mathbf{x}}'^T(n)\hat{\mathbf{x}}'(n) + P_k(n)}, \quad (27)$$

where μ_1 is the fixed step-size parameter. It is shown in [23] that the term $P_k(n)$ in (27) plays a very important role. In the case of perturbation term in the error signal of ANC filter, step-size decreases to a small value thus preventing ANC system from divergence. The weight update equation for $\hat{\mathbf{s}}(n)$ is given as

$$\hat{\mathbf{s}}(n+1) = \hat{\mathbf{s}}(n) + \mu_s(n)f(n)\mathbf{v}_g(n), \quad (28)$$

where $\mathbf{v}_g(n) = [v_g(n), v_g(n-1), \dots, v_g(n-L_s+1)]^T$ is the input signal vector, and $\mu_s(n)$ is normalized step-size parameter for $\hat{\mathbf{s}}(n)$ being computed as

$$\mu_s(n) = \frac{\mu_2}{\mathbf{v}_g^T(n)\mathbf{v}_g(n) + P_{\hat{y}'(n)}}, \quad (29)$$

TABLE I
DETAILED COMPUTATIONAL COMPLEXITY ANALYSIS FOR VARIOUS METHODS DISCUSSED IN THE PAPER. (FOR EACH METHOD, CORRESPONDING NUMBER (FROM FIRST COLUMN) OF EQUATION IS GIVEN AT THE END OF THE TABLE)

S.No	To compute	×	+	÷	√
1	$v_g(n) - y(n) = v_g(n) - \mathbf{w}^T(n)\mathbf{x}(n)$	L_w	L_w		
2	$\hat{\mathbf{x}}'(n) = \hat{\mathbf{s}}^T(n)\mathbf{x}(n)$	L_s	$L_s - 1$		
3	$\hat{v}_g'(n) = \hat{\mathbf{s}}^T(n)v_g(n)$	L_s	$L_s - 1$		
4	$f(n) = e(n) - \hat{v}_g'(n)$	—	1		
5	$\mathbf{w}(n+1) = \mathbf{w}(n) + \mu_w e(n)\hat{\mathbf{x}}'(n)$	$L_w + 1$	L_w		
6	$\hat{\mathbf{s}}(n+1) = \hat{\mathbf{s}}(n) + \mu_s f(n)v_g(n)$	$L_s + 1$	L_s		
	Computations in Eriksson's method ^a [8] Total:	$2L_w + 3L_s + 2$	$2L_w + 3L_s - 1$		
7	$v_g(n) = G(n)v(n)$	1	—		
8	$\hat{y}'(n) = \hat{\mathbf{s}}^T(n)\mathbf{y}(n)$	L_s	$L_s - 1$		
9	$\hat{d}'(n) = \mathbf{w}^T(n)\hat{\mathbf{x}}'(n)$	L_w	$L_w - 1$		
10	$\hat{d}(n) = f(n) + \hat{y}'(n)$ and $k(n) = \hat{d}(n) - \hat{d}'(n)$	—	2		
11	$P_e(n), P_f(n)$ using (5)	$3 \times 2 = 6$	$1 \times 2 = 2$		
12	$\rho(n) = \frac{P_f(n)}{P_e(n)}$	—	—	1	
13	$\mu_s(n) = \rho(n)\mu_{s_{\min}} + (1 - \rho(n))\mu_{s_{\max}}$	2	2		
14	$G(n) = \sqrt{\rho(n)\sigma_{\max}^2 + (1 - \rho(n))\sigma_{\min}^2}$	2	1	—	1
15	$\mathbf{w}(n+1) = \mathbf{w}(n) + \mu_w k(n)\hat{\mathbf{x}}'(n)$	$L_w + 1$	L_w		
16	$\hat{\mathbf{s}}(n+1) = \hat{\mathbf{s}}(n) + \mu_s(n)f(n)v_g(n)$	$L_s + 1$	L_s		
	Computations in Akhtar's method ^b [15] Total:	$3L_w + 4L_s + 13$	$3L_w + 4L_s + 4$	1	1
17	$v_g(n-D) - y(n) = v_g(n-D) - \mathbf{w}^T(n)\mathbf{x}(n)$	L_w	L_w		
18	$\hat{v}_g'(n) = \hat{\mathbf{s}}_A^T(n)v_{g(L_s+D)}(n)$	$L_s + D$	$L_s + D - 1$		
19	$\ \hat{\mathbf{s}}_0(n)\ ^2 = \hat{\mathbf{s}}_0^T(n)\hat{\mathbf{s}}_0(n)$	D	$D - 1$		
20	$\ v_{g(L_s+D)}(n)\ ^2 = \mathbf{v}_{g(L_s+D)}^T(n)v_{g(L_s+D)}(n)$	$(L_s + D)$	$L_s + D - 1$		
21	$\hat{N}_s(n) = \lambda\hat{N}_s(n-1) + [(1-\lambda)(\hat{\mathbf{s}}_0^T(n)\hat{\mathbf{s}}_0(n)) + (\mathbf{v}_{g(L_s+D)}^T(n)v_{g(L_s+D)}(n))/D]$	3	1	1	
22	$\frac{\hat{N}_s(n)}{P_f(n)} > \mu_{s_{\min}}$ in (10)	—	—	1	
23	$\mu_s(n) = \frac{\hat{N}_s(n)}{(P_f(n)v_{g(L_s+D)}^T(n)v_{g(L_s+D)}(n))}$ OR $\mu_s(n) = \frac{\mu_{s_{\min}}}{\mathbf{v}_{g(L_s+D)}^T(n)v_{g(L_s+D)}(n)}$	—	—	1	
24	$\ \hat{\mathbf{x}}'(n)\ ^2 = \hat{\mathbf{x}}'^T(n)\hat{\mathbf{x}}'(n)$	L_w	$L_w - 1$		
25	$\hat{\mathbf{m}}(n) = \lambda\hat{\mathbf{m}}(n-1) + \frac{(1-\lambda)k(n)\hat{\mathbf{x}}'(n)}{\hat{\mathbf{x}}'^T(n)\hat{\mathbf{x}}'(n)}$	$2L_w + 1$	L_w	1	
26	$\hat{N}_w(n) = \lambda\hat{N}_w(n-1) + (1-\lambda)k(n)\hat{\mathbf{m}}^T(n)\hat{\mathbf{x}}'(n)$	$L_w + 2$	L_w		
27	$\mu_w(n) = \frac{\hat{N}_w(n)}{P_k(n)(\hat{\mathbf{x}}'^T(n)\hat{\mathbf{x}}'(n))}$	1	—	1	
28	$P_s(n) = \lambda P_s(n-1) + (1-\lambda)\hat{\mathbf{s}}^T(n)\hat{\mathbf{s}}(n)$	$L_s + 2$	L_s		
29	$G(n) = \sqrt{\frac{P_e(n)}{(R(n)+1)P_s(n)}}$	1	—	1	1
30	$\mathbf{w}(n+1) = \mathbf{w}(n) + \mu_w(n)k(n)\hat{\mathbf{x}}'(n)$	$L_w + 1$	L_w		
31	$\hat{\mathbf{s}}_A(n+1) = \hat{\mathbf{s}}_A(n) + \mu_s(n)f(n)v_{g(L_s+D)}(n)$	$L_s + D + 1$	$L_s + D$		
	Computations in Carini's method ^c [17] Total:	$7L_w + 6L_s + 4D + 19$	$6L_w + 6L_s + 4D - 1$	6	1
32	$P_x(n), P_v(n), P_k(n), P_{y'}(n)$ using (5)	$3 \times 4 = 12$	$3 \times 4 = 4$		
33	$P_{f_d}(n) = \lambda P_{f_d}(n-1) + (1-\lambda)f(n)f(n-1)$	2	1		
34	$\gamma(n) = \rho(n)\gamma_{\min} + (1-\rho(n))\gamma_{\max}$	3	1		
35	$\beta(n) = \alpha\beta(n-1) + \gamma(n)(P_{f_d}(n)/P_v(n))^2$	3	1	1	
36	(for $P_f(n) > P_x(n)$), $G(n) = \sqrt{\frac{P_f(n-1)}{\ \hat{\mathbf{s}}(n)\ ^2}}$ (for $P_f(n) \leq P_x(n)$), $G(n) = \sqrt{\frac{P_x(n)}{P_v(n)}}$ OR $G(n) = \beta(n)$	L_s	$L_s - 1$	1	1
37	$\ v_g(n)\ ^2 = \mathbf{v}_g^T(n)v_g(n)$	L_s	$L_s - 1$		
38	$\mu_s(n) = \frac{\mu_1}{\mathbf{v}_g^T(n)v_g(n) + P_{y'}(n)}$	—	1	1	
39	$\mu_w(n) = \frac{\mu_2}{\hat{\mathbf{x}}'^T(n)\hat{\mathbf{x}}'(n) + P_k(n)}$	—	1	1	
40	$\mathbf{w}(n+1) = \mathbf{w}(n) + \mu_w(n)k(n)\hat{\mathbf{x}}'(n)$	$L_w + 1$	L_w		
41	$\hat{\mathbf{s}}(n+1) = \hat{\mathbf{s}}(n) + \mu_s(n)f(n)v_g(n)$	$L_s + 1$	L_s		
	Computations in the proposed method ^d Total:	$4L_w + 6L_s + 29$ $4L_w + 5L_s + 29$	$4L_w + 6L_s + 7$ $4L_w + 5L_s + 6$	5 5	1 1

^aEriksson's method: 1-6; ^bAkhtar's method: 1-4, 7-16; ^cCarini's method: 2, 4, 7-11, 17-31; ^dProposed method: 1-4, 7-12, 24, 32-41.

where μ_2 is another fixed step-size parameter, and the term $P_{y'}(n)$ (estimated using estimator like (5)) is employed to have some upper bound on $\mu_s(n)$. This upper bound in (29) is needed

to avoid the possibility of very large step-size value, when the term $\mathbf{v}_g^T(n)v_g(n)$ becomes very small in steady-state due to the proposed gain scheduling.

TABLE II
COMPUTATIONAL COMPLEXITY COMPARISON (COMPUTATIONS PER ITERATION) OF VARIOUS METHODS DISCUSSED IN THE PAPER. THE VALUE OF FILTER TAP-WEIGHT LENGTHS AND DELAY, IN THREE DIFFERENT SCENARIOS, ARE GIVEN AT THE END OF TABLE

	Total computations	Example 1 ^a	Example 2 ^b	Example 3 ^c
Eriksson's method [8]	$4L_w + 6L_s + 1$	225	4097	10241
Akhtar's method [15]	$6L_w + 8L_s + 19$	339	5651	14355
Carini's method [17]	$13L_w + 12L_s + 8D + 25$	697	10009	26649
Proposed method				
(for $P_f(n) > P_x(n)$)	$8L_w + 12L_s + 42$	490	8234	20522
(for $P_f(n) \leq P_x(n)$)	$8L_w + 10L_s + 41$	457	7209	18473

^a $L_w = 32, L_s = 16, D = 8$; ^b $L_w = 256, L_s = 512, D = 64$; ^c $L_w = L_s = 1024, D = 128$.

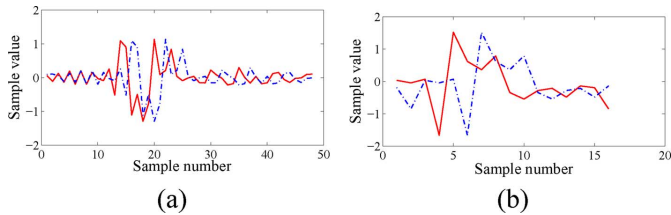


Fig. 5. Impulse response of (a) Primary path with impulse response vector $\mathbf{p}(n)$, (b) Secondary path with impulse response vector $\mathbf{s}(n)$. (solid, and dashed-dotted curves show, respectively, original, and perturbed acoustic paths.).

D. Computational Complexity Analysis

A detailed computational complexity analysis for the proposed method in comparison with Eriksson, Akhtar, and Carini methods is given in Table I. In Eriksson's method, fixed step-sizes are employed for both the adaptive filters, and no gain scheduling ($G(n) = 1$) is employed, therefore Eriksson's method has the lowest computational cost as compared with other methods. The Carini's method has the highest computational cost among all methods discussed in this paper. The main reason for an increased computational cost is the online estimation of optimal normalized step-size parameters. Akhtar's method uses a fixed step-size for $\mathbf{w}(n)$, a VSS for $\hat{\mathbf{s}}(n)$, and a gain scheduling strategy to improve the noise-reduction performance. Akhtar's method has lower computational cost as compared with Carini's and the proposed methods. The proposed method has a higher computational cost as compared to Eriksson's and Akhtar's methods; however, the proposed method does offer some computational saving as compared with the Carini's method. This saving in computations is due to the use of the normalized step-size parameters instead of optimal normalized step-size parameter. The difference in the computations between Carini's and the proposed method becomes very significant for filters with long tap-weight lengths. For clarity of presentation, Table II shows numerical examples for total computations required per iteration for various methods.

IV. SIMULATION RESULTS

In this section, simulation results are presented to compare the performance of the proposed method with Akhtar's [15], and Carini's method [17]. The performance comparison is carried out on the basis of following performance measures.

TABLE III
SIMULATION PARAMETERS FOR VARIOUS METHODS DISCUSSED IN PAPER

Parameters	
Akhtar's method [15]	$\mu_w = 5 \times 10^{-4}, \mu_{s_{\min}} = 1 \times 10^{-3},$ $\mu_{s_{\max}} = 1 \times 10^{-2}, \sigma_{\min}^2 = 1 \times 10^{-3},$ $\sigma_{\max}^2 = 0.1.$
Carini's method [17]	$\mu_{s_{\min}} = 4 \times 10^{-3}, D = 8,$ $\lambda = 0.6, R(n) = 1.$
Proposed method	$\mu_1 = 3 \times 10^{-1}, \mu_2 = 8 \times 10^{-2},$ $\alpha = 0.997, \gamma_{\min} = 0.3, \gamma_{\max} = 0.9.$

- Relative modeling error of secondary path being defined as

$$\Delta S(n)(\text{dB}) = 10 \log_{10} \frac{\|\mathbf{s}(n) - \hat{\mathbf{s}}(n)\|^2}{\|\mathbf{s}(n)\|^2}. \quad (30)$$

- Mean-squared error (MSE) at the error microphone, $E[e^2(n)]$.
- Steady-state value of the time-varying gain, $G(n)$.

Using data from [1], the acoustic paths $\mathbf{p}(n)$ and $\mathbf{s}(n)$ are modeled as FIR filters of tap-weight lengths 48 and 16, respectively. The impulse response of $\mathbf{p}(n)$ and $\mathbf{s}(n)$ are shown in Fig. 5. The adaptive filters $\mathbf{w}(n)$, $\hat{\mathbf{s}}(n)$, and $\hat{\mathbf{s}}_A(n)$ are selected as FIR filters of tap-weight length 32, 16 and $16 + D$ respectively. The value of D and other simulation parameters are given in Table III. The selection of step-size parameter for adaptive filter depends upon the adaptation method, power of input signal of adaptive filter (except for NLMS algorithm), and the power of interference term in the error signal of the adaptive filter. The adaptation strategies for ANC filter and SPM filter in Akhtar's, Carini's, and the proposed methods are different. In addition to this, a different gain scheduling strategy results in different power of input signal for $\hat{\mathbf{s}}(n)$, and different power of the interference term in the error signal $k(n)$ of ANC filter, therefore, the step-size parameters are tuned for each method to achieve the fast and stable convergence of the adaptive filters. In all methods, the adaptive filter weights are initialized by null vectors (in the proposed method $\hat{\mathbf{s}}(n)$ and in Carini's method $\hat{\mathbf{s}}_0(n)$ are initialized by all ones). The power of the auxiliary noise $v(n)$ is set to 1. The value of forgetting factor λ is chosen as 0.99. The sampling frequency is selected as 2 kHz. All the simulation results are averaged over 20 independent realizations.

For stable operation of MFXNLMS algorithm based ANC system the phase error between $\mathbf{s}(n)$ and $\hat{\mathbf{s}}(n)$ must be within

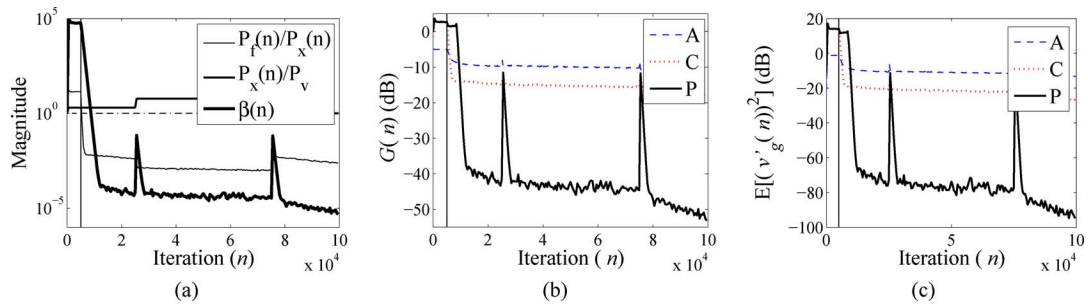


Fig. 6. Simulation results in Case 1: (a) Variation of $P_f(n)/P_x(n)$, $P_x(n)/P_v$, and $\beta(n)$ in the proposed method. (b) The time-varying gain $G(n)$ (dB). (c) The mean-squared auxiliary noise, $E[(v'_g(n))^2]$ (dB) (A=Akhtar's method; C=Carini's method; P=Proposed method).

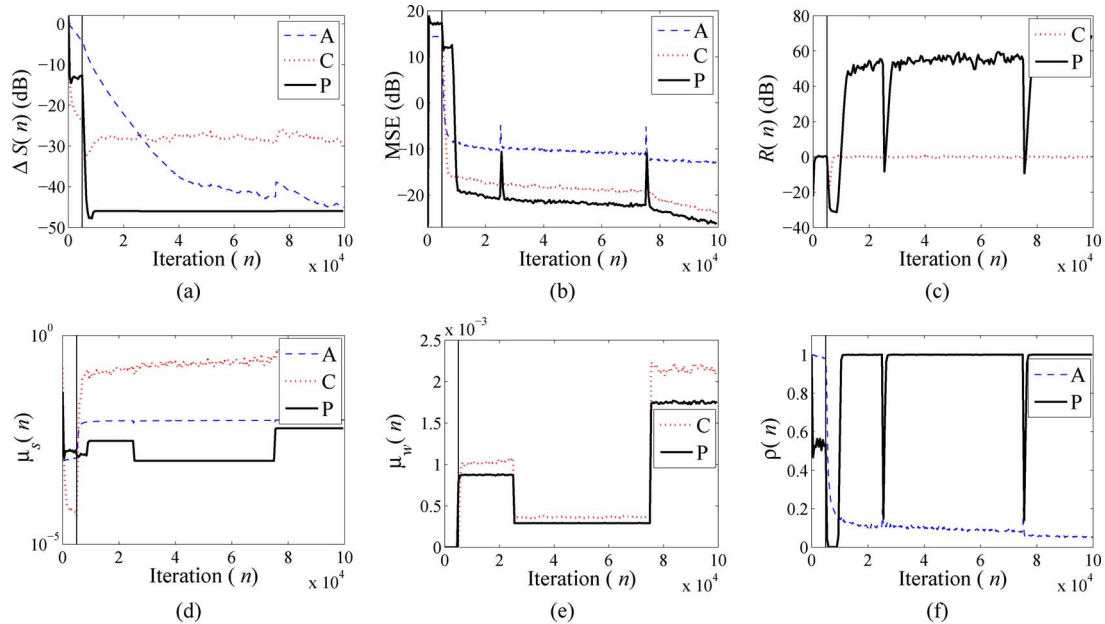


Fig. 7. Simulation results in Case 1: (a) The relative modeling error, $\Delta S(n)$ (dB). (b) The mean-squared error $E[(e^2(n))]$ (dB). (c) The ratio $R(n)$ (dB). (d) The time-varying step-size parameter $\mu_s(n)$. (e) The time-varying step-size parameters $\mu_w(n)$. (f) The variation of the parameter $\rho(n)$ as defined in (24) (A=Akhtar's method; C=Carini's method; P=Proposed method).

the bound of $\pm 90^\circ$ [3]–[7]. Since the secondary path $s(n)$ is unknown, therefore offline modeling ($d(n) = 0$) of the secondary path can be used to satisfy the $\pm 90^\circ$ bound at the start-up of ANC system. The other option (with $d(n)$ present) is to keep ANC filter in sleep state for a while and only the modeling filter $\hat{s}(n)$ is adapted. In this paper, the second option is used and ANC filter is in sleep state from $n = 0$ to $n = 5000$ as done in [16], and [17]. In all plots for simulation results, the vertical line at $n = 5000$ marks the end of this phase.

A. Case 1: Multi-Tonal Input With Time-Varying Power

In this case, the reference signal, $x(n)$, is a multi-tonal input with frequencies 100, 200, 300, and 400 Hz. Initially variance of $x(n)$ is selected as 2, and then changed to 6, and 1 at iteration $n = 25000$, and $n = 75000$, respectively. A WGN with zero-mean and variance 0.002 is added to $x(n)$ to account for any measurement noise. The simulation results for Case 1 are presented in Figs. 6 and 7.

- Fig. 6(a) shows the plots for $P_f(n)/P_x(n)$, $P_x(n)/P_v$, and $\beta(n)$. These time-varying quantities are involved in the selection of (17) or (18) for gain $G(n)$. The horizontal

line (dashed-dotted) with amplitude 1 is plotted as a reference line to show that as long as $P_f(n) > P_x(n) \Rightarrow P_f(n)/P_x(n) > 1$, (17) is used for computing $G(n)$. It is found from Fig. 6(a) that from $n = 0$ to $n = 5247$ the ratio $P_f(n)/P_x(n) > 1$, therefore (17) is used for $G(n)$. After $n = 5247$ the condition $P_f(n)/P_x(n) > 1$ is false and the $G(n)$ is computed using (18). It is clear from Fig. 6(a) that at the start of second stage ($P_f(n)/P_x(n) \leq 1$) of gain scheduling strategy the value of $\beta(n)$ is greater than $P_x(n)/P_v$ and the gain is determined by the input reference signal power, otherwise the gain follows the variation of $\beta(n)$. After convergence of the ANC system the change in the variance of the input reference signal, $x(n)$, changes the error signal $f(n)$, therefore causing a change in $P_{f_d}(n)$ and $\beta(n)$.

- The plot for the time-varying gain $G(n)$ is shown in Fig. 6(b). In Akhtar's method the value of $\rho(n)$ is never zero, and hence $G(n)$ is higher in steady-state. In Carini's method the gain is determined by $E[(d(n) - y'(n))^2]$ in all operating conditions, while in the proposed method the gain, at steady-state, is varied on the basis of the correlation estimate of the two adjacent values of the error

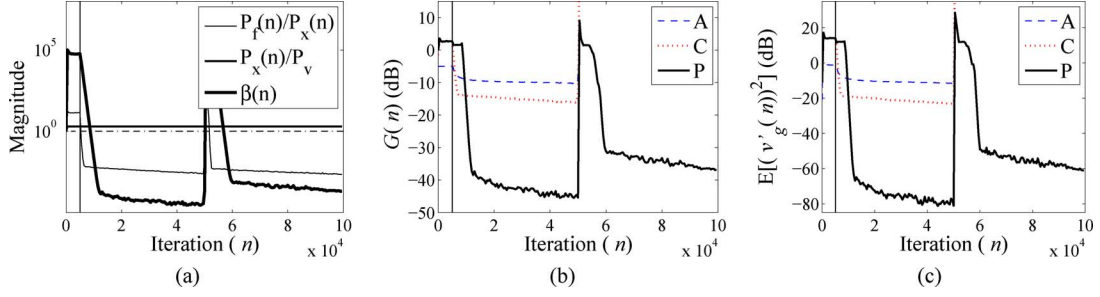


Fig. 8. Simulation results in Case 2: (a) Variation of $P_f(n)/P_x(n)$, $P_x(n)/P_v$, and $\beta(n)$ in the proposed method. (b) The time-varying gain $G(n)$ (dB). (c) The mean-squared auxiliary noise, $E[(v'_g(n))^2]$ (dB) (A=Akhtar's method; C=Carini's method; P=Proposed method).

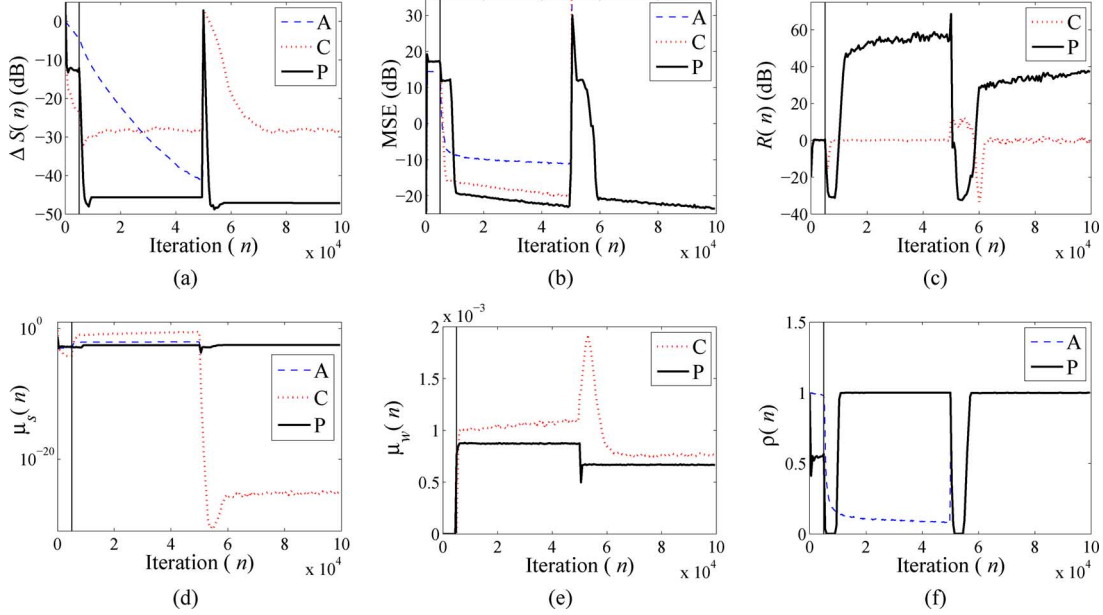


Fig. 9. Simulation results in Case 2: (a) The relative modeling error, $\Delta S(n)$ (dB). (b) The mean-squared error $E[(e^2(n))]$ (dB). (c) The ratio $R(n)$ (dB). (d) The time-varying step-size parameter $\mu_s(n)$. (e) The time-varying step-size parameters $\mu_w(n)$. (f) The variation of the parameter $\rho(n)$ as defined in (24) (A=Akhtar's method; C=Carini's method; P=Proposed method).

signal $f(n)$ of SPM filter. This results in a much smaller steady-state value of $G(n)$ as compared to that of Carini's method. After convergence of ANC system the change in the variance of the input reference signal $x(n)$ changes the signal $f(n)$, therefore causing a change in $G(n)$.

- As $E[(v'_g(n))^2] = G^2(n)\|s(n)\|^2$, so a small value of the gain $G(n)$ results in a small ANP at the error microphone. The curves for the mean-square value of the auxiliary noise at the error microphone are shown in Fig. 6(c). The change in the variance of $x(n)$ changes $P_f(n)$. The change in $P_f(n)$ causes a change in $G(n)$ and therefore changes $E[(v'_g(n))^2]$.
- Fig. 7(a) shows the plot of relative modeling error $\Delta S(n)$, as defined in (30). To explain the fast convergence of the SPM filter in the proposed method consider $n \geq 5247$ where the gain $G(n)$ is computed using (18). As stated earlier, as long as in the second stage of gain scheduling the value of $\beta(n) > P_x(n)/P_v$ the gain is determined by the input reference signal power and is higher than Akhtar's and Carni's methods (see Fig. 6(b)). This large value of the gain $G(n)$ results in a large power of input signal, $E[(v'_g(n))^2]$, for $\hat{s}(n)$ and hence a large value for $E[e^2(n)]$. This results in the fast convergence of the SPM

filter $\hat{s}(n)$. It is shown in [14] that after the convergence of ANC system the norms of the adaptive filters $\hat{s}(n)$ and $w(n)$ are almost not affected with changes in input reference signal power. In Fig. 7(a), we observe that there is no change in $\Delta S(n)$ in the proposed method even when the variance of the input reference signal $x(n)$ changes.

- In Fig. 7(b) MSE curves are plotted for various methods. For changes in the input reference signal variance at iterations $n = 25000$ and $n = 75000$, the value of $E[e^2(n)]$ in the proposed method is almost same as in Carini's methods. When ANC system is in transient stage or when the acoustic paths are perturbed, in both these situation fast convergence of $\hat{s}(n)$ is desirable. The proposed gain scheduling scheme is such that as far as $\hat{s}(n)$ is away from $s(n)$ the ratio $R(n) < 0$ dB, $E[(v'_g(n))^2] > E[(d(n) - y'(n))^2]$ and hence resulting in large $E[e^2(n)]$ in transient stage, and in situations when acoustic paths are perturbed. We observe that the proposed method improves steady-state noise-reduction performance as compared to the existing methods. The reason for an improved noise-reduction performance is the proposed strategy for gain scheduling which results in a small contribution of $E[(v'_g(n))^2]$ in $E[e^2(n)]$ at steady-state.

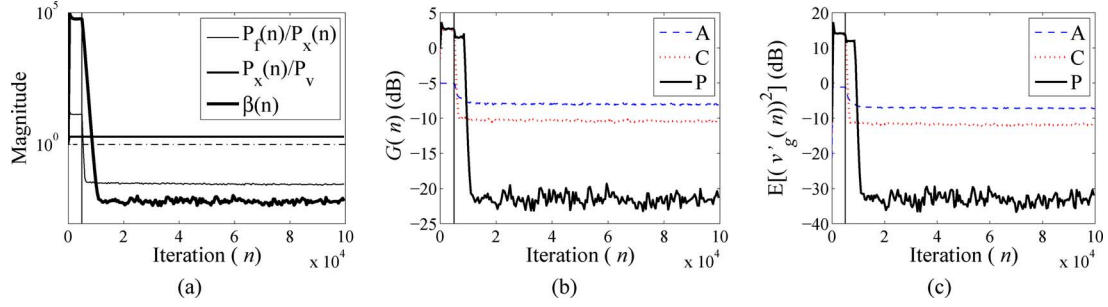


Fig. 10. Simulation results in Case 3: (a) Variation of $P_f(n)/P_x(n)$, $P_x(n)/P_v$, and $\beta(n)$ in the proposed method. (b) The time-varying gain $G(n)$ (dB). (c) The mean-squared auxiliary noise, $E[(v'_g(n))^2]$ (dB) (A=Akhtar's method; C=Carini's method; P=Proposed method).

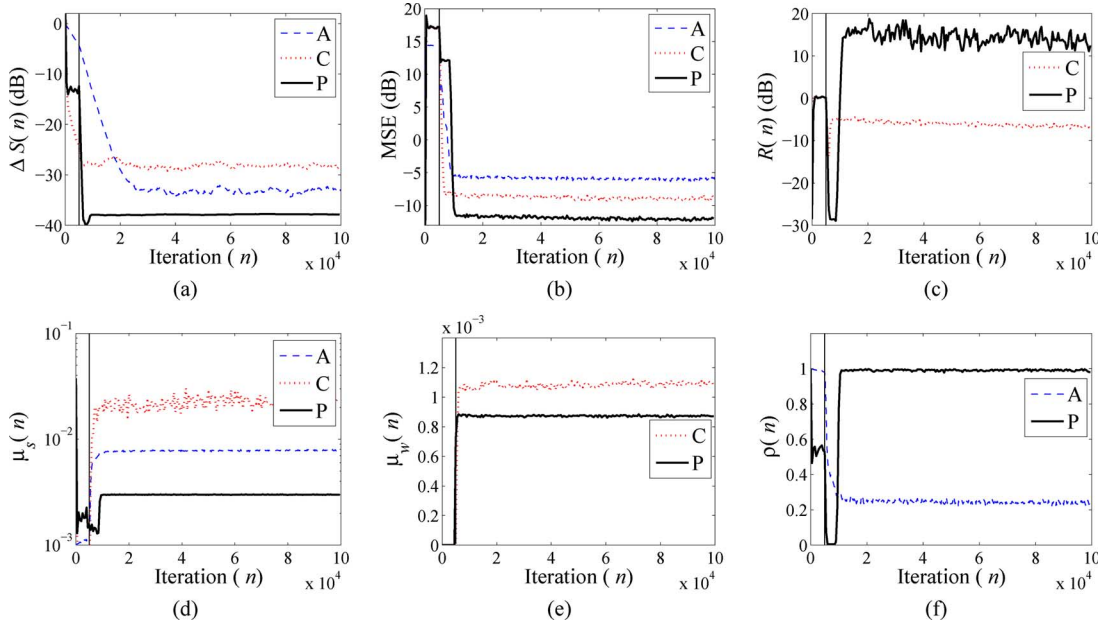


Fig. 11. Simulation results in Case 3: (a) The relative modeling error, $\Delta S(n)$ (dB). (b) The mean-squared error $E[(e^2(n))]$ (dB). (c) The ratio $R(n)$ (dB). (d) The time-varying step-size parameter $\mu_s(n)$. (e) The time-varying step-size parameters $\mu_w(n)$. (f) The variation of the parameter $\rho(n)$ as defined in (24) (A=Akhtar's method; C=Carini's method; P=Proposed method).

- The variation of $R(n)$ in the Carini's and the proposed methods is shown in Fig. 7(c). It is clear that ratio $R(n) = \text{constant} \quad \forall n$ in Carini's method, whereas $R(n)$ is allowed to vary in the proposed method. As long as $\hat{\mathbf{s}}(n)$ is away from $\mathbf{s}(n)$, $R(n) < 0$ dB, and $R(n) > 0$ dB as $\hat{\mathbf{s}}(n)$ converges to $\mathbf{s}(n)$. After ANC system converges, the change in the variance of input reference signal results in an increase in the gain $G(n)$. The increase in $G(n)$ causes the value of $E[(v'_g(n))^2]$ to increase and therefore the value of $R(n)$ decreases.
- The time-varying step-size for SPM filter, $\mu_s(n)$, in Akhtar's, Carini's and the proposed methods is plotted in Fig. 7(d). In Akhtar's method, the step-size $\mu_s(n)$ is set to a minimum value at the start-up and later increased to a maximum value. In Carini's method the variation of step-size $\mu_s(n)$ depends upon the distance of $\hat{\mathbf{s}}_0(n)$ from $[0, 0, \dots, 0]^T$, and the step-size $\mu_s(n)$ increases because of decrease of term $\mathbf{v}_{g(L_s+D)}^T(n)\mathbf{v}_{g(L_s+D)}(n)$ in the denominator of (10).
- The time-varying step-size for ANC filter, $\mu_w(n)$, is plotted in Fig. 7(e). As the normalization factor is in-

involved in computing $\mu_w(n)$, therefore the large input signal power results in small step-size and vice versa.

- Fig. 7(f) shows the variation of $\rho(n)$ in Akhtar's and the proposed methods. In Akhtar's method the value of $\rho(n)$ decrease from one to zero, whereas in the proposed method the value of $\rho(n)$ is almost one in steady-state.

B. Case 2: Multi-Tonal Input and Strong Acoustic Path Perturbation

The existing methods work fine for slight variations in the acoustic paths. In actual practice significant changes in the acoustic paths may be encountered due to the movement of the error microphone or the loudspeaker. In this case study a strong perturbation in the acoustic paths is simulated by giving two sample right circular shift to the truncated impulse responses of $\mathbf{p}(n)$ and $\mathbf{s}(n)$. The impulse response of perturbed primary and secondary acoustic paths are shown (by dashed-dotted line) in Fig. 5. The simulation results for this case study are presented in Figs. 8 and 9, where jumps at $n = 5 \times 10^4$ indicate a perturbation in the acoustic paths.

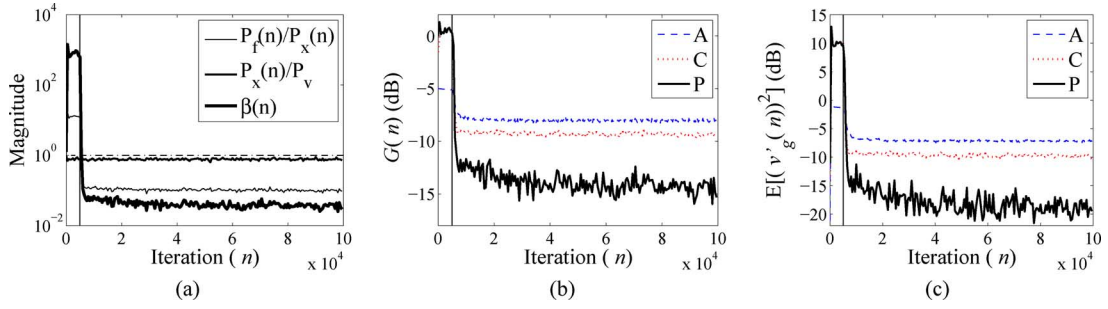


Fig. 12. Simulation results in Case 4: (a) Variation of $P_f(n)/P_x(n)$, $P_x(n)/P_v$, and $\beta(n)$ in the proposed method. (b) The time-varying gain $G(n)$ (dB). (c) The mean-squared auxiliary noise, $E[(v'_g(n))^2]$ (dB) (A=Akhtar's method; C=Carini's method; P=Proposed method).

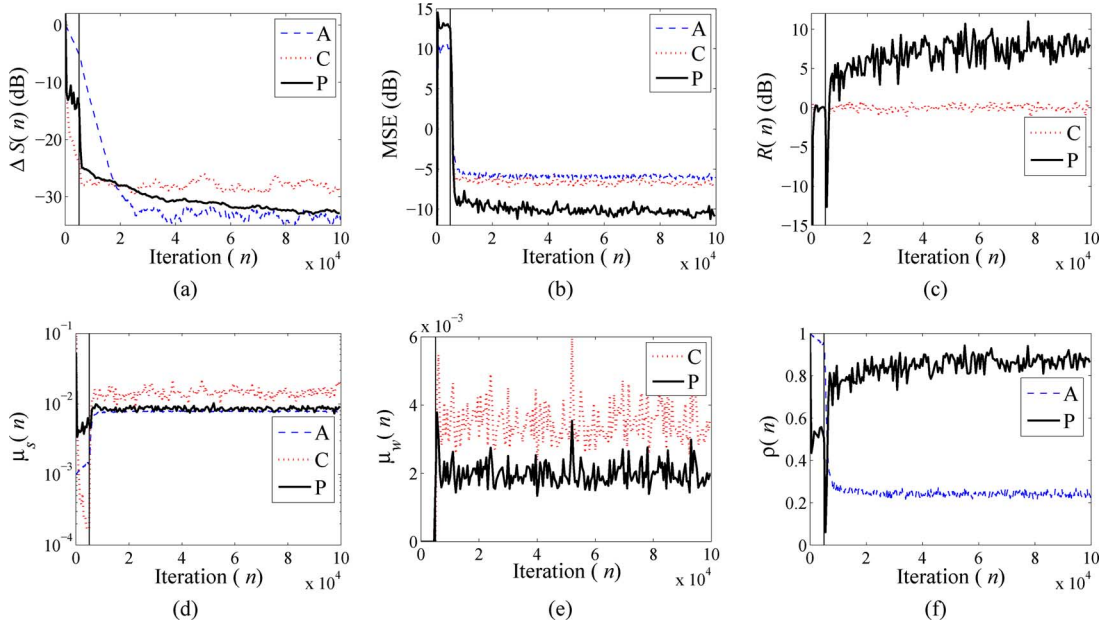


Fig. 13. Simulation results in Case 4: (a) The relative modeling error, $\Delta S(n)$ (dB). (b) The mean-squared error $E[(e^2(n))]$ (dB). (c) The ratio $R(n)$ (dB). (d) The time-varying step-size parameter $\mu_s(n)$. (e) The time-varying step-size parameters $\mu_w(n)$. (f) The variation of the parameter $\rho(n)$ as defined in (24) (A=Akhtar's method; C=Carini's method; P=Proposed method).

- From Fig. 8(a), it is clear that just before the acoustic paths perturbation the gain in the proposed method is following the variations of $\beta(n)$, and is computed using (18). The perturbation in acoustic paths results in $P_f(n) > P_x(n)$ and the gain is computed using (17) until the condition $P_f(n) > P_x(n)$ is false.
- The variation of the gain $G(n)$ is shown in Fig. 8(b). In Akhtar's method, the gain $G(n)$ is not able to increase in accordance with the power of the interference term $E[(d(n) - y'(n))^2]$, so the strong perturbation results in a large interference $(d(n) - y'(n))$ in the error signal $f(n)$ of SPM filter, resulting in the divergence of SPM and hence the overall ANC system. In Carini's method, the step-size $\mu_w(n)$ jumps to higher value after perturbation (see Fig. 9(e)). The large value of the step-size in the presence of a strong perturbation term $(v'_g(n) - \hat{v}'_g(n))$ results in the divergence of ANC filter, thus resulting in very large value of $E[(d(n) - y'(n))^2]$. To keep the ratio $R(n) = 0$ dB, the gain $G(n)$ also increases to a very large value. Only the proposed method is convergent and gain

$G(n)$ reduces to a small value even after the perturbation in the acoustic paths.

- Fig. 8(c) shows the plot of $E[(v'_g(n))^2]$. As expected, a large value of $G(n)$ results in a large value of $E[(v'_g(n))^2]$ and vice versa.
- Fig. 9(a) show the curves for $\Delta S(n)$. In the proposed method a fast convergence of the SPM filter is obtained before and after the acoustic path perturbation. The reason for the fast convergence is the same as explained in Case 1. The fast convergence of SPM filter quickly neutralizes the effect of the perturbation term $(v'_g(n) - \hat{v}'_g(n))$ from the error signal $k(n)$ of ANC filter $w(n)$, and thus the ANC system remains stable even for a strong perturbation in the acoustic paths. The behavior of $\Delta S(n)$ for Carini's method is quite interesting. The ANC filter is diverged, but the modeling filter still manages to converge. The reason is quite simple, a large value of $E[(d(n) - y'(n))^2]$ results in a large $E[(v'_g(n))^2]$ to keep the ratio $R(n)$ constant, thus resulting in a very small step-size (see Fig. 9(d) for variation in $\mu_s(n)$). A very small value of the step-size

allows SPM filter to converge even for a very strong perturbation term $(d(n) - y'(n))$ in the error signal $f(n)$ of SPM filter.

C. Case 3: Multi-Tonal Input and the Uncorrelated WGN at Error Sensor

In this case study a zero-mean WGN $v_s(n)$ with variance 0.05; uncorrelated with the reference and auxiliary noise; is assumed to be present at the error microphone. The noise at the error microphone contributes to the residual error signal $e(n)$, thus the gain in Carini's method (see (4)) will be higher as compared with the gain for $v_s(n) = 0$. This large value of the gain $G(n)$ results in $E[(v'_g(n))^2] > E[(d(n) - y'(n))^2]$, thus making $R(n) < 0$ dB $\forall n$. In the proposed method the gain $G(n)$ in steady-state depends upon $\beta(n)$, however $\beta(n)$ itself depends upon the estimate of autocorrelation of $f(n)$ and $f(n-1)$, therefore the gain $G(n)$ is independent of error sensor noise $v_s(n)$ (see (21)).

The simulation results for Case 3 are shown in Figs. 10 and 11, where we observe that the performance of the proposed method is better than the existing methods in terms of modeling accuracy of the SPM filter, the power of the residual error signal at the error microphone, and steady-state value of the time-varying gain $G(n)$.

D. Case 4: Broad-Band Input

The practical example of the broad-band feed-forward ANC system is the control of acoustic noise in long, narrow ducts, such as exhaust pipes and ventilation systems [1]. The objective of this case study is to compare the performance of the proposed algorithm for broad-band input reference signal $x(n)$. The signal $x(n)$ is generated by filtering a WGN signal with variance 2 through a bandpass FIR filter of order 128 with a passband of [100 500] Hz. A WGN with a zero-mean and variance 0.002 is added to account for the measurement noise. The simulation results for Case 4 are shown in Figs. 12 and 13. As in previous cases, the proposed method performs better than the existing methods.

V. CONCLUSION

In this paper, we propose a new two-stage strategy for gain scheduling to vary the ANP in ANC systems with online SPM. The proposed strategy improves the noise-reduction performance of the ANC system in steady-state, which is the ultimate goal of the ANC system. In addition to this, when the ANC system is far from steady-state, the proposed strategy gives fast convergence of the SPM filter. The fast convergence of SPM filter makes the proposed method more robust against strong perturbations in the acoustic paths. Furthermore, the proposed method works well even in the presence of uncorrelated disturbance at the error microphone. In steady-state the gain in the proposed method is determined by the estimate of the autocorrelation of present and previous sample value of the error signal of SPM filter. This estimate is independent of the uncorrelated disturbance at the error microphone. In the proposed method, the ANC and SPM filters are adapted using normalized step-sizes which reduces the computational

requirements. The main advantage of the proposed method is the robust performance even in the case of strong perturbation in the acoustic paths.

The robustness of the proposed method against errors in the SPM filter tap-weight length has not been studied. The detailed study of the effects of different tap-weight length of $\hat{s}(n)$ on the performance of ANC system is beyond the scope of this paper. In addition to this, the detailed convergence analysis of ANC system with proposed gain scheduling strategy is a task for future research.

ACKNOWLEDGMENT

The authors would like to thank anonymous reviewers for providing many insightful comments on both the original and the revised versions of the manuscript. This has greatly improved the overall organization and quality of presentation.

REFERENCES

- [1] S. M. Kuo and D. R. Morgan, *Active Noise Control Systems-Algorithms and DSP Implementation*. New York: Wiley, 1996.
- [2] S. Elliot, *Signal Processing for Active Control (Signal Processing and its Applications)*. London, U.K.: Academic, 2000.
- [3] D. R. Morgan, "An analysis of multiple correlation cancellation loops with a filter in the auxiliary path," *IEEE Trans. Acoust., Speech, Signal Process.*, vol. ASSP-28, no. 4, pp. 454-467, Aug. 1980.
- [4] S. J. Elliott, I. M. Stotbers, and P. A. Nelson, "A multiple error LMS algorithm and its application to the active control of sound and vibration," *IEEE Trans. Acoust., Speech, Signal Process.*, vol. ASSP-35, no. 10, pp. 1423-1434, Oct. 1987.
- [5] C. C. Boucher, S. J. Elliott, and P. A. Nelson, "Effect of errors in the plant model on the performance of algorithms for adaptive feedforward control," in *Proc. Inst. Elect. Eng.*, 1991, vol. 138, pp. 313-319.
- [6] S. D. Snyder and C. H. Hansen, "The effect of transfer function estimation errors on the filtered-X-LMS algorithm," *IEEE Trans. Signal Process.*, vol. 42, no. 4, pp. 950-953, Apr. 1994.
- [7] M. Wu, X. Qiu, and G. Chen, "The statistical behavior of phase error for deficient-order secondary path modeling," *IEEE Signal Process. Lett.*, vol. 15, pp. 313-316, 2008.
- [8] L. J. Eriksson and M. C. Allie, "Use of random noise for online transducer modeling in an adaptive active attenuation system," *J. Acoust. Soc. Amer.*, vol. 85, pp. 797-802, Feb. 1989.
- [9] C. Bao, P. Sas, and H. V. Brussel, "Adaptive active control of noise in 3-D reverberant enclosure," *J. Sound Vibr.*, vol. 161, no. 3, pp. 501-514, Mar. 1993.
- [10] S. M. Kuo and D. Vijayan, "A secondary path modeling technique for active noise control systems," *IEEE Trans. Speech Audio Process.*, vol. 5, no. 4, pp. 374-377, Jul. 1997.
- [11] M. Zhang, H. Lan, and W. Ser, "Cross-updated active noise control system with online secondary path modeling," *IEEE Trans. Speech Audio Process.*, vol. 9, no. 5, pp. 598-602, Jul. 2001.
- [12] M. T. Akhtar, M. Abe, and M. Kawamata, "A new variable step size LMS algorithm-based method for improved online secondary path modeling in active noise control systems," *IEEE Trans. Audio, Speech Lang. Process.*, vol. 12, no. 2, pp. 720-726, Mar. 2006.
- [13] D. Cornelissen and P. C. Sommen, "New online secondary path estimation in a multipoint filtered-x algorithm for acoustic noise canceling," in *Proc. IEEE ProRIS 99*, 1999, pp. 97-103.
- [14] M. Zhang, H. Lan, and W. Ser, "A robust online secondary path modeling method with auxiliary-noise-power scheduling strategy and norm constraint manipulation," *IEEE Trans. Speech Audio Process.*, vol. 11, no. 1, pp. 45-53, Jan. 2003.
- [15] M. T. Akhtar, M. Abe, and M. Kawamata, "Noise power scheduling in active noise control systems with online secondary path modeling," *IEICE Electron. Express*, vol. 4, no. 2, pp. 66-71, 2007.
- [16] A. Carini and S. Malatini, "Auxiliary noise power scheduling for feed-forward active noise control," in *Proc. ICASSP '08, Int. Conf. Acoust., Speech, Signal Process.*, Las Vegas, NV, 2008, pp. 341-344.

- [17] A. Carini and S. Malatini, "Optimal variable step-size NLMS algorithms with auxiliary noise power scheduling for feedforward active noise control," *IEEE Trans. Audio, Speech Lang. Process.*, vol. 16, no. 8, pp. 1383–1395, Nov. 2008.
- [18] J. Liu, Y. Xiao, J. Sun, and L. Xu, "Analysis of online secondary-path modeling with auxiliary noise scaled by residual noise signal," *IEEE Trans. Audio, Speech Lang. Process.*, vol. 18, no. 8, pp. 1978–1993, Nov. 2010.
- [19] P. Davari and H. Hassanpour, "Designing a new robust online secondary path modeling technique for feedforward active noise control systems," *Signal Process.*, vol. 89, pp. 1195–1204, Jun. 2009.
- [20] S. Ahmed, A. Oishi, M. T. Akhtar, and W. Mitsuhashi, "Auxiliary noise power scheduling for online secondary path modeling in single channel feedforward active noise control systems," in *Proc. ICASSP '12, Int. Conf. Acoust., Speech, Signal Process.*, Kyoto, Japan, Mar. 2012, pp. 317–320.
- [21] S. Yamamoto and S. Kitayama, "An adaptive echo canceller with variable step gain method," *Trans. IEICE Japan*, vol. E65, no. 1, pp. 1–8, Jan. 1982.
- [22] T. Aboulnasr and K. Mayyas, "A robust variable step-size LMS-type algorithm: Analysis and simulations," *IEEE Trans. Signal Process.*, vol. 45, pp. 631–639, Mar. 1997.
- [23] J. E. Greenberg, "Modified LMS algorithm for speech processing with an adaptive noise canceller," *IEEE Trans. Speech Audio Process.*, vol. 6, no. 4, pp. 338–351, Jul. 1998.



Shakeel Ahmed (S'12) received the B.S. degree in electrical engineering from NWFP University of Engineering and Technology Peshawar, Pakistan in 2005, MS degree in systems engineering from Pakistan Institute of Engineering and Applied Sciences, Islamabad, Pakistan, under a fellowship programme in 2007. He is currently pursuing his Ph.D. degree under a Japanese government (MEXT) scholarship. His research interests include adaptive signal processing for active noise control systems.



Muhammad Tahir Akhtar (M'05–SM'12) received the B.S. degree in electrical engineering from the University of Engineering and Technology, Taxila, Pakistan, in 1997, the M.S. degree in systems engineering from Quaid-i-Azam University, Islamabad, Pakistan, in 1999 (through a fellowship from Pakistan Institute of Engineering and Applied Sciences (PIEAS), Islamabad, Pakistan), and the Ph.D. degree in electronic engineering from Tohoku University, Sendai, Japan, in 2004 (through Japanese Government Scholarship). He is currently a specially appointed Assistant Professor at the Center for Frontier Science and Engineering (CFSE), University of Electro-Communications, Tokyo, Japan, and a Special Visiting Researcher at The Center for Research and Development of Educational Technology (CRADLE), Tokyo Institute of Technology, Tokyo, Japan. He was a visiting researcher at ISVR, University of Southampton, UK (Dec. 2008 – Feb. 2009), and at INC, University of California San Diego (Nov. 2010 – Mar. 2011), with funding from Japan society for promotion of sciences under the grant "Institutional Programme for Young Researcher Overseas Visits". His research interests include adaptive signal processing, active noise control, blind source separation, and biomedical signal processing.

Dr. Akhtar won the Best Student Paper at the IEEE 2004 Midwest Symposium on Circuits and Systems, Hiroshima, Japan, and student paper award (with Marko Kanadi) at the 2010 RISP International Workshop on Nonlinear Circuits, Communications and Signal Processing. He is member of The European Association for Signal Processing (EURASIP), and the Asia-Pacific Signal and Information Processing Association (APSIPA). Since 2011, he has been serving as a co-editor for APSIPA newsletter.



Xi Zhang (M'94–SM'01) received the B.E. degree in electronics engineering from the Nanjing University of Aeronautics and Astronautics (NUAA), Nanjing, China, in 1984 and the M.E. and Ph.D. degrees in communication engineering from the University of Electro-Communications (UEC), Tokyo, Japan, in 1990 and 1993, respectively. He was with the Department of Electronics Engineering at NUAA from 1984 to 1987, and with the Department of Communications and Systems at UEC from 1993 to 1996, all as an Assistant Professor. He was with the Department of Electrical Engineering at Nagaoka University of Technology (NUT), Niigata, Japan, as an Associate Professor, from 1996 to 2004. Currently, he is with the Department of Communication Engineering and Informatics at UEC, as a Professor. He was a Visiting Scientist of the MEXT of Japan with the Massachusetts Institute of Technology (MIT), Cambridge, from 2000 to 2001. His research interests are in the areas of digital signal processing, filter design theory, filter banks and wavelets, and its applications to image and video coding.

Dr. Zhang is a senior member of the IEICE of Japan. He received the third prize of the Science and Technology Progress Award of China in 1987, and the challenge prize of Fourth LSI IP Design Award of Japan in 2002. He served as an Associate Editor for the IEEE SIGNAL PROCESSING LETTERS from 2002 to 2004.